

# Energy Efficiency Analysis of UAV-Assisted mmWave HetNets

Syed Naqvi\*, Jacob Chakareski\*, Nicholas Mastronarde†, Jie Xu◊, ‡Fatemeh Afghah, †Abolfazl Razi  
 \*University of Alabama, †University of Buffalo, ◊University of Miami, ‡Northern Arizona University

**Abstract**—We study downlink transmission in a multi-band heterogeneous network comprising unmanned aerial vehicle (UAV) small base stations and ground-based dual mode mmWave small cells within the coverage area of a microwave ( $\mu W$ ) macro base station. We formulate a two-layer optimization framework to simultaneously find efficient coverage radius for the UAVs and energy efficient radio resource management for the network, subject to minimum quality-of-service (QoS) and maximum transmission power constraints. The outer layer derives an optimal coverage radius/height for each UAV as a function of the maximum allowed path loss. The inner layer formulates an optimization problem to maximize the system energy efficiency (EE), defined as the ratio between the aggregate user data rate delivered by the system and its aggregate energy consumption (downlink transmission and circuit power). We demonstrate that at certain values of the target SINR  $\tau$  introducing the UAV base stations doubles the EE. We also show that an increase in  $\tau$  beyond an optimal EE point decreases the EE.

## I. INTRODUCTION

5G heterogeneous networks (HetNets) will comprise a mix of network tiers of different sizes, transmission powers, backhaul connections, and radio access technologies [1]. The use of drone small cells or wireless aerial platforms has been proposed recently to improve network coverage and capacity [2]. Additionally, UAVs are expected to prove instrumental for public safety and disaster management [3]. We consider a heterogeneous network comprising a microwave macro base station (BS), multiple ground-based dual-mode mmWave small BS (SBS), and multiple microWave-operating aerial (UAV) BS, as illustrated in Figure 1. Related UAV work has largely

leveraged the LoS probability expression from [6]. Now, despite demonstrating promising performance in extending network coverage, there are still several operational challenges of UAV BS, ranging from energy limitations and interference management to optimal 3D deployment, which merit further investigation. For instance, [7] determines the optimal UAV altitude to minimize transmitted power required to cover a target region. [8] extends this work by determining the optimal UAV locations given their corresponding cell boundaries are known. However, both studies do not consider ground-based small and macro cells existing simultaneously. Furthermore, [9] studies proactive deployment of cache-enabled UAVs for optimizing a given QoE metric, determining user-UAV associations, the optimal UAV locations, and the cached content.

Another feature of 5G networks is the use of mmWave and microWave resources simultaneously. The utilization of mmWave technology has recently gained attention due to the higher available bandwidth (in the range of 1–2 GHz) and the possibility of larger antenna arrays due to the smaller wavelength of mmWave signals [10]. The authors in [11] present a novel scheduling framework for small cells operating in dual mode, i.e., in both mmWave and ultra high frequency (UHF) bands. We adopt a similar approach towards transmissions from the SBS, whereby the users in the small cell may utilize one of the two frequency bands available in the mmWave band, depending on which one maximizes their respective rate. In contrast to related work [7, 12], we study for the first time the EE of a UAV-assisted multi-band HetNet, comprising ground-based macro BS and dual-mode mmWave SBS, and derive an optimization framework to maximize it. We propose a joint subcarrier and power allocation scheme to maximize the system EE while satisfying a minimum QoS level for the users and a maximum power transmission constraint. To solve this radio resource management problem, we propose a two-layer optimization framework. In its inner layer, the EE of the macro BS tier is maximized. In its outer layer, the power consumption of the UAV tier is optimized to satisfy its users' minimum rate requirement, while limiting its maximum interference to the macro BS tier.

The rest of this paper is organized as follows. Section II presents our system models, formulating the considered infrastructure and air-to-ground channels. Sections III-V formulate the power allocation mechanisms for the  $\mu W$  BS, the UAVs, and the SBS, respectively. In Section VI, we present our experimental results. Section VII concludes the paper.

## II. SYSTEM MODEL

The network comprises a macro cell BS,  $W$  SBS, and  $E$  UAV BS, with a total of  $M$  users distributed randomly in the region of interest. The macro cell BS is denoted as

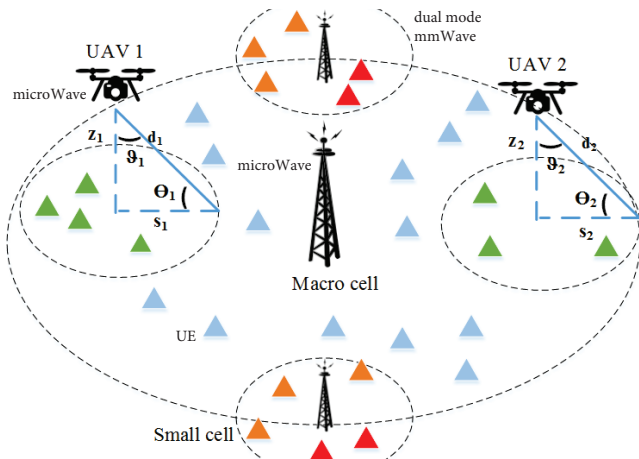


Fig. 1: The investigated system model.

dealt with air-to-ground channel modeling, investigating line-of-sight (LoS) probability and path loss [4, 5]. In our work,

The work of S. Naqvi and J. Chakareski has been supported in part by NSF awards CCF-1528030 and ECCS-1711592. The work of N. Mastronarde has been supported in part by NSF award ECCS-1711335.

$\mu W$ . Each UAV and the  $\mu W$  BS share  $N_{\mu W}$  subcarriers, whereas each mmWave SBS  $w$  has two available mmWave bands  $b \in \{H, L\}$  where  $H$  and  $L$  denote the higher/lower mmWave bands. We consider  $H$  and  $L$  to be respectively noise and interference limited, as indicated by [13]. Each user is expected to achieve a minimum data rate  $R_{\min}$ . It should be noted that all BS in the three-tier hybrid HetNet operate independently to find their optimal transmission power in a distributed manner [14]. We assume that each subcarrier can be exclusively assigned to only one user within the same BS of each tier  $k$ . We assume that each user  $m$  associates to the tier  $k$  with the maximum biased received power  $\Gamma_m^k = \frac{\beta_k P_k^{\max} G(\theta_k)}{\text{PL}_m^k}$ , where  $P_k^{\max}$  is the maximum transmission power of tier  $k$ ,  $\beta_k$  is the biasing factor of tier  $k \in \{\text{macro, UAV, small}\}$ ,  $\theta_k$  is the azimuthal angle of the BS beam alignment,  $\text{PL}_m^k$  is the average downlink path loss experienced by user  $m$  when served by tier  $k$  (one of its BS), and  $G(\theta_k)$  is the respective antenna gain. Based on this user association scheme, user  $m$  can belong to one of the following three disjoint sets: (i)  $m$  is served by the macro BS tier or the small cell tier's mmWave band  $L$ , (ii)  $m$  is served by the UAV tier, or (iii)  $m$  is served by small cell tier's mmWave band  $H$ . With respect to downlink transmission, the objective is to maximize the system EE in the case of (i), to minimize the power consumption in the case of (ii), and to maximize the transmission rate in the case of (iii). The achievable rate of user  $m$  on subcarrier  $n$  associated with tier  $l \in \{\text{macro, UAV}\}$  is

$$r_{m,n}^{(l)} = \Theta_l B_l \log_2(1 + \gamma_{m,n}^{(l)} \times p_{m,n}^{(l)}), \quad (1)$$

where  $\Theta_l$  is the proportion of bandwidth allocated to each subcarrier by the associated BS of tier  $l$ ,  $B_l$  denotes the total bandwidth available to the associated BS of tier  $l$ ,  $p_{m,n}^{(l)}$  denotes the power allocated to user  $m$  on subcarrier  $n$  by this BS, and  $\gamma_{m,n}^{(l)}$  is the respective (downlink) channel gain.

The distance  $d$  between user  $m$  and its associated UAV  $e$  is

$$d = \sqrt{(x - x_e)^2 + (y - y_e)^2 + z_e^2}, \quad (2)$$

where  $x_e$ ,  $y_e$  and  $z_e$  represent the  $x$ ,  $y$  and  $z$  coordinates of a UAV  $e$  in a cartesian plane. The altitude of the UAV  $e$  is  $z_e = s_e \tan(\theta_e)$ , where  $s_e$  is the 2D distance of  $m$  from  $e$  and  $\theta_e = \pi/2 - \vartheta$ , for  $\vartheta$  the UAV's half beamwidth angle. Similarly, the LoS probability between  $e$  and  $m$  is given as  $P_{\text{LoS}} = 1/(1 + C \cdot \exp[-Y(\theta_e - C)])$  [6], where  $C$  and  $Y$  are constants dependent on the environment settings (rural, urban, dense urban, or others).

#### A. Dual Mode mmWave Small Cells

We consider that the SBS are using TDMA. The average achievable rate of user  $m$  on subcarrier  $n$  associated with the mmWave tier on band  $b$  across  $T$  time slots is,

$$r_{m,n}^{w,b} = \frac{1}{T} \sum_{t=1}^T \Theta_{w,b} B_{w,b} \log_2(1 + \gamma_{m,n_t}^{w,b} \times p_{m,n_t}^{w,b}), \quad (3)$$

where  $\Theta_{w,b}$  is the bandwidth share allocated to each subcarrier on band  $b$ ,  $B_{w,b}$  indicates the total bandwidth available to

the mmWave SBS on band  $b$ , and  $p_{m,n_t}^{w,b}$  indicates the power allocated to user  $m$  on the subcarrier  $n_t$  at time slot  $t$ . Thus, the total achieved rate of user  $m$  associated with SBS  $w$  is  $r_{m,n}^w = \sum_{b \in \{H,L\}} r_{m,n}^{w,b}$ . Finally, the total data rate for user  $m$ , associated with either  $\mu W$  BS, UAV BS, or  $w$  SBS is

$$\overline{R}_m = \sum_{k \in \{l,w\}} \sum_{n=1}^{N_k} \sigma_{m,k} r_{m,n}^{(k)}, \quad (4)$$

where  $\sigma_{m,k} = 1$ , if  $m$  is associated with tier  $k$ , and 0 otherwise, and  $N_k$  is the total number of subcarriers available to tier  $k$ .

We denote the total power consumed by user  $m$  as  $\overline{P}_m = \sum_{k \in \{l,w\}} \sum_{n=1}^{N_k} \sigma_{m,k} p_{m,n}^{(k)}$ . Then, we define the system EE as  $\sum_{m=1}^M \overline{R}_m / (\sum_{m=1}^M \overline{P}_m + \sum_{k \in K} P_{C_k})$ , where  $P_{C_k}$  is the circuit power of tier  $k$ .

#### B. Determining the optimal altitude of a UAV

We determine the UAV  $e$ 's height above ground such that its maximum path loss experienced at transmission (to its farthest user) does not exceed  $\text{PL}_{\max}$ . In particular, we first characterize the path loss between  $e$  and its associated users as

$$\Omega_\varrho(\text{dB}) = 20 \log \left( \frac{4\pi}{\lambda_{\mu W}} \right) + 10\alpha_e \log(d) + \eta_\varrho + \chi_\varrho^{\mu W},$$

where  $\varrho \in \{\text{LoS, NLoS}\}$ ,  $\eta_{\text{LoS}}$  and  $\eta_{\text{NLoS}}$  denote the average additional loss in LoS or NLoS links relative to the free space propagation loss measured in dB,  $\alpha_e$  is the path loss exponent for UAV  $e$ , and  $\chi^{\mu W}$  represents the shadowing in the microwave band (in dB), modeled as a Gaussian random variable with zero mean and variance  $\xi_1^2$ . We then formulate the average path loss between  $e$  and its associated user  $m$  as  $\text{PL}_m^e = P_{\text{LoS}} \times \Omega_{\text{LoS}} + P_{\text{NLoS}} \times \Omega_{\text{NLoS}}$ , where  $P_{\text{NLoS}} = 1 - P_{\text{LoS}}$ .

Finally, given the above, we first derive  $\text{PL}_{\max}$  as

$$\text{PL}_{\max} = d^{\alpha_e} [P_{\text{LoS}}(10^{0.1 \times \eta_{\text{LoS}}}) + P_{\text{NLoS}}(10^{0.1 \times \eta_{\text{NLoS}}})], \quad (5)$$

where  $d$  in this case denotes the distance to the farthest served user. Subsequently, we can derive  $z_e$  from  $\text{PL}_{\max}$  as

$$z_e = \cos(\vartheta) \frac{\text{PL}_{\max}}{[P_{\text{LoS}}(10^{0.1 \times \eta_{\text{LoS}}}) + P_{\text{NLoS}}(10^{0.1 \times \eta_{\text{NLoS}}})]}. \quad (6)$$

### III. POWER ALLOCATION MECHANISM FOR $\mu W$ BS

Our objective here is to simultaneously optimize the achievable rate and EE of all users associated with the  $\mu W$  BS subject to a maximum transmission power constraint and minimum required QoS level. The joint optimization is equivalent to maximizing the sum rate and minimizing the total power consumption for the users. We formulate it as a multi-objective problem which we then transform into a single objective optimization using the weighted sum method by normalizing the two objectives by  $R_{\text{norm}}$  and  $P_{\text{norm}}$ , respectively, to ensure a consistent comparison, as shown below:

$$\max_{\mathbf{P}} \phi \frac{\sum_{m \in M_{\mu W}} \sum_{n \in N_{\mu W}} \kappa_{m,n} r_{m,n}^{(\mu W)}}{R_{\text{norm}}} - (1 - \phi) \frac{P}{P_{\text{norm}}}, \quad (7)$$

$$\text{subject to: } \sum_{m \in M_{\mu W}} \sum_{n \in N_{\mu W}} p_{m,n}^{(\mu W)} \leq P_{\mu W}^{\max},$$

$$R_m \geq R_{\min}, \forall m, p_{m,n}^{(\mu W)} \geq 0, \kappa_{m,n} \in \{0, 1\}, \forall m, n,$$

where  $M_{\mu W}$  denotes the total number of users associated with  $\mu W$  BS,  $N_{\mu W}$  denotes the total number of subcarriers available to this BS,  $P_{\text{norm}}$  is the maximum transmit power of the BS,  $R_{\text{norm}}$  is the maximum achievable rate corresponding to  $P_{\text{norm}}$ ,  $P = \sum_{m,n} p_{m,n}^{(\mu W)}$ , and  $\kappa_{m,n}$  indicates whether subcarrier

$n$  has been assigned to user  $m$ . We note that while the user association has been done beforehand, we use the subscript  $\mu W$  to improve the readability here. Since user  $m$  can share at most one subcarrier with another user associated with a UAV BS, we can decompose (7) into (i) a power allocation problem for users associated with the  $\mu W$  BS and a UAV, and (ii) a subcarrier allocation problem for the users associated with the  $\mu W$  BS. We formulate the first problem as

$$\max_{\mathbf{p}} \phi \frac{\sum_{m \in M_{\mu W}} \sum_{n \in N_{\mu W}} r_{m,n}^{(\mu W)}}{R_{\text{norm}}} - (1 - \phi) \frac{P}{P_{\text{norm}}}, \quad (8)$$

subject to the first three constraints in (7).

We note that when  $\phi = 1$ , (8) transforms into rate maximization, while for  $\phi = 0$  it transforms into power minimization. Moreover, for  $\phi = \phi_{\text{EE}} \in [0, 1]$ , it transforms into EE maximization. We write the Lagrangian function for (8) as

$$T(\mathbf{p}, \boldsymbol{\mu}, \boldsymbol{\varphi}) = \frac{\phi}{R_{\text{norm}}} \sum_{m,n} r_{m,n}^{(\mu W)} - \frac{(1 - \phi)}{P_{\text{norm}}} P +$$

$$\boldsymbol{\mu} \left( P_{\mu W}^{\max} - \sum_{m,n} p_{m,n}^{(\mu W)} \right) + \sum_{m \in M_{\mu W}} \varphi_m (R_m - R_{\min}),$$

where  $P_{\mu W}^{\max}$  is the maximum transmit power of the  $\mu W$  BS.

The optimal value  $p_{m,n}^{(\mu W)}$  can then be computed as

$$p_{m,n}^{(\mu W)} = \left[ \frac{\left( \frac{\phi}{R_{\text{norm}}} + \varphi_m \right) \Theta_{\mu W} B_{\mu W}}{\left( \mu + \frac{1 - \phi}{P_{\text{norm}}} \right) (\ln 2)} - \frac{1}{\gamma_{m,n}^{(\mu W)}} \right]^+, \quad (9)$$

where  $\mu$  and  $\varphi_m$  are the Lagrangian multipliers associated with the first two constraints in (7), which we update using a sub-gradient method as follows:

$$\mu_{\mu W}(j+1) = \left[ \mu_{\mu W}(j) - s_1 \left( P_{\mu W}^{\max} - \sum_{m=1}^{M_{\mu W}} \sum_{n=1}^{N_{\mu W}} p_{m,n}^{(\mu W)} \right) \right]^+,$$

$$\varphi_m(j+1) = [\varphi_m(j) - s_2 (R_m - R_{\min})]^+, \quad (10)$$

where  $[x]^+ = \max(0, x)$ . Algorithm 1 provides an algorithmic description of the formulated power allocation mechanism. Using  $p_{m,n}^*$  as the optimal power allocation solution to (8), for the users associated with the  $\mu W$  BS, we model the subcarrier allocation problem as

$$\max_{\kappa_{m,n}} \sum_{m,n} \kappa_{m,n} p_{m,n}^*, \text{ s.t. } \kappa_{m,n} \in \{0, 1\}, \forall m, n. \quad (11)$$

---

#### Algorithm 1 Power allocation for users of $\mu W$ BS

---

- 1: Set  $j = 0$  and  $j_{\max} = 10^4$ ; Initialize  $p_{m,n}^{(\mu W)} = 10^{-6}$ ,  $\varphi_m = 10^{-2}$ ,  $\forall m$ , and  $\mu_{\mu W} = 10^{-2}$ .
  - 2: **while**  $\varphi_m$  and  $\mu_{\mu W}$  have not converged or  $j < j_{\max}$  **do**
  - 3:   Compute  $p_{m,n}^{(\mu W)}$  using (9)
  - 4:   Update  $\mu_{\mu W}(j+1)$  and  $\varphi_m(j+1)$  using (10)
  - 5: **end while**
  - 6: End
- 

We solve (11) using the Hungarian method [15], which is a combinatorial optimization algorithm that solves assignment problems efficiently (in polynomial time).

#### IV. POWER ALLOCATION MECHANISM FOR UAVS

To guarantee QoS to users associated with the  $\mu W$  BS, we impose a maximum interference threshold constraint  $I_t$  such that the total cross-tier interference caused by the UAV to the user associated with the  $\mu W$  BS and sharing the same subcarrier should always be less than or equal to  $I_t$ . The transmission power on a reused subcarrier by the UAV should be chosen such that the  $\mu W$  BS users can satisfy their minimum rate requirement. We calculate this power from

$$\log_2 \left( 1 + \frac{p_{m,n}^{(\mu W)} |h_{m,n}^{(\mu W)}|^2}{\left( \sigma^2 + \frac{p_{m,n}^e}{\text{PL}_m^e} |h_{m,n}^{(e)}|^2 \right) \text{PL}_m^{\text{macro}}} \right) \geq R_{\min},$$

$$\Rightarrow p_{m,n}^e \leq \frac{\text{PL}_m^e}{|h_{m,n}^{(e)}|^2} \left( \frac{p_{m,n}^{(\mu W)} |h_{m,n}^{(\mu W)}|^2}{(2^{R_{\min}} - 1) \text{PL}_m^{\text{macro}}} - \sigma^2 \right),$$

where  $h_{m,n}^{(l)}$  denotes the squared envelope of the multi-path fading between user  $m$  and the associated BS of tier  $l$  (macro or UAV),  $\sigma^2$  is the thermal noise power,  $p_{m,n}^e$  is the transmission power of UAV  $e$  to user  $m \in M_e$  on subcarrier  $n$ , which it shares with  $\mu W$  BS user  $m \in M_{\mu W}$ ,  $p_{m,n}^{(\mu W)}$  is the transmission power of the  $\mu W$  BS at the given subcarrier  $n$  to user  $m \in M_{\mu W}$ ,  $\text{PL}_m^e$  is the path loss between UAV  $e$  and user  $m \in M_e$ , and  $R_{\min}$  is the user minimum rate requirement.

Similarly, the transmission power of UAV  $e$  to user  $m \in M_e$  on subcarrier  $n$  based on the predetermined interference threshold  $I_t$  can be computed as  $\bar{p}_{m,n}^e \leq \frac{I_t \text{PL}_m^e}{|h_{m,n}^{(e)}|^2}$ , where  $\text{PL}_m^e$  is the path loss experienced between UAV  $e$  and the user  $m \in M_{\mu W}$  sharing the same subcarrier  $n$ .

Finally, the minimum transmission power that UAV  $e$  needs to use to meet the minimum rate requirement is

$$p_{m,n}^{e,\min} = \frac{\text{PL}_m^e}{|h_{m,n}^{(e)}|^2} (2^{R_{\min}} - 1) \left( \sigma^2 + \frac{p_{m,n}^{(\mu W)} |h_{m,n}^{(\mu W)}|^2}{\text{PL}_m^e} \right), \quad (12)$$

where  $\text{PL}_m^e$  is the path loss between UAV  $e$  and its associated user  $m \in M_e$ . Hence, the final constrained transmission power of UAV  $e$  to user  $m$  on subcarrier  $n$  is,

$$p_{m,n}^{e,\text{opt}} = \begin{cases} \min(\bar{p}_{m,n}^e, \max(p_{m,n}^e, p_{m,n}^{e,\min})) & \text{if } \Lambda \geq p_{m,n}^{e,\min} \\ \text{Infeasible} & \text{otherwise,} \end{cases}$$

where  $\Lambda = \min(p_{m,n}^e, \bar{p}_{m,n}^e)$ .

## V. POWER/SUBCARRIER ALLOCATION FOR MMWAVE SBS

The SBS have the flexibility to serve their users on one of the available two mmWave bands  $\{L, H\}$ . As noted earlier, band  $H$  is assumed to be noise limited whereas the lower mmWave band  $L$  is assumed to be interference limited considering the co-tier interference among the SBS operating on this band. For band  $H$ , each subcarrier  $n \in N_{w,H}$  is allocated transmission power  $p_{m,n}^{w,H} = P_w^{\max}/N_{w,H}$ , where  $P_w^{\max}$  is the maximum transmit power of SBS  $w$  and  $N_{w,H}$  is the total number of subcarriers available at SBS  $w$  on band  $H$ .

As the users served by SBS  $w$  on the lower band  $L$  experience co-tier interference from the neighbouring mmWave SBS, there is a need for efficient power control. Similarly to the mechanism described in Section III, the transmission power of SBS  $w$  operating on band  $L$  to user  $m$  on subcarrier  $n \in N_{w,L}$  can be computed as

$$p_{m,n}^{w,L} = \left[ \frac{\left( \frac{\phi}{R_{\text{norm}}} + \varphi_m \right) \Theta_{w,L} B_{w,L}}{\left( \mu_w + \frac{1-\phi}{P_{\text{norm}}} \right) (\ln 2)} - \frac{1}{\gamma_{m,n}^{(w)}} \right]^+$$

Subcarrier pairing in the small cells operating on band  $H$  (noise limited regime) in TDMA is performed so as to allocate  $T$  combinations of subcarriers to each user which maximize their average achieved rate across  $T$  time slots. On the other hand, the small cells operating on band  $L$  (interference limited regime) allocate  $T$  combinations of subcarriers to each user to maximize their average achieved EE across  $T$  time slots. We omit here the detailed procedure for subcarrier pairing in dual-mode mmWave small cells in TDMA, to conserve space.

## VI. PERFORMANCE EVALUATION

In our experiments, we consider a hybrid cellular network comprising one  $\mu W$  BS coexisting with three dual mode mmWave SBS and two UAV BS. We consider 50 users uniformly distributed in a square geographical area  $1 \text{ km} \times 1 \text{ km}$ . The mmWave SBS are randomly deployed on the macro cell edge to cater to cell edge users. We consider a 2 GHz carrier frequency for both the  $\mu W$  and UAV BS. The carrier frequencies for the SBS are 28 GHz ( $L$  band) and 73 GHz ( $H$  band). The bandwidth of both  $\mu W$  and UAV BS is 20 MHz. The SBS bandwidth is 1 GHz ( $L$  band) and 2 GHz ( $H$  band).

The maximum transmission power of  $\mu W$  BS, UAVs, and SBS are 46 dBm, 30 dBm, and 30 dBm. The total number of subcarriers available to each tier  $k$  is 128. The path loss exponent for the ground user-UAV link is 2 while that for  $\mu W$  BSs is 3. The LoS and NLoS pathloss exponents for mmWave small cells are 2 and 3.3 [10]. The minimum rate requirement is set to 3 b/s/Hz unless otherwise stated. The thermal noise is assumed to be -174 dBm/Hz. The half power beamwidth angle for mmWave small cell is  $10^\circ$  [10] and the shadowing in  $\mu W$  BS or UAVs are considered to be 4 dB whereas the shadowing in mmWave small cells are 5.2 dB and 7.2 dB for LoS and NLoS links [16]. All statistical results are calculated

over various channel conditions and user locations averaged over  $10^3$  Monte Carlo iterations.

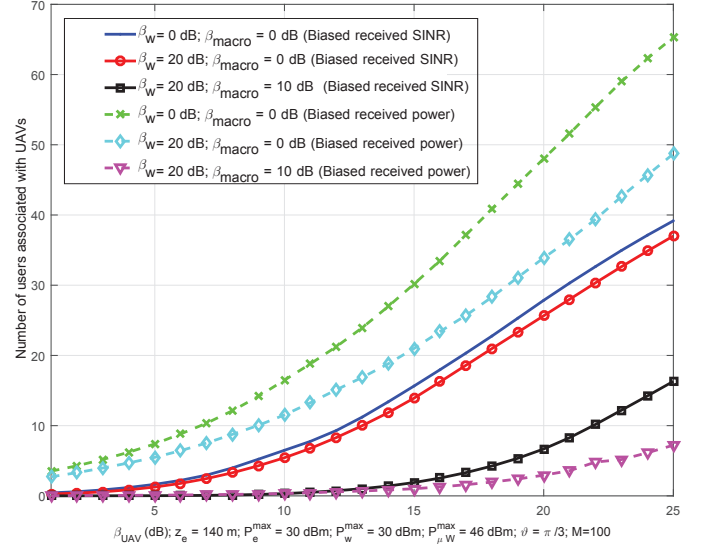


Fig. 2: User association for the UAV tier versus  $\beta_{\text{UAV}}$  based on biased received power and SINR.

Figure 2 depicts the number of users associated with the UAV tier for increasing  $\beta_{\text{UAV}}$  (biasing factor), on the basis of biased received power using  $\Gamma_m^k$  and biased SINR. The six graphs in the figure represent various biasing scenarios for the SBS and the  $\mu W$  BS. When the biasing factors for both the mmWave SBS and the  $\mu W$  BS are 0 dB, it yields the greatest number of users associated with the UAV tier, irrespective of whether the association is done on the basis of biased received power or biased SINR. In fact, for the case when biasing is performed based on the received power, increasing  $\beta_{\text{UAV}}$  from 10 dB to 15 dB causes an increase by approximately 67% in the number of users associated with the UAV tier. The graphs representing the cases when both the SBS and the UAV have non-zero biasing factors show a similar increasing trend. However, the cumulative number of users associated with the UAV tier remains lower than that for the previous case, as a greater number of users are now associated with the mmWave tier. As the maximum transmission power of the  $\mu W$  BS is the highest among all the tiers, therefore, introducing a non-zero biasing factor  $\beta_{\text{macro}}$  causes a sharp decline in the number of users associated with the UAV tier irrespective of the type of user association. The figure shows that at  $\beta_{\text{UAV}} = 25$  dB, there is a nearly 84% decrease in the number of users utilizing the UAV tier when  $\beta_{\text{UAV}} = 10$  dB, relative to when only the SBS biasing factor is taken to be non-zero.

The impact of the half power beam-width angle of the UAV,  $\vartheta$ , on the number of users associated with the UAV tier is shown in Figure 3. User association is done on the basis of biased received power. All three curves demonstrate a general decrease with an increase in  $\vartheta$ . This is due to the fact that an increase in  $\vartheta$  causes a decrease in the elevation angle,  $\theta_e$ , resulting in a small coverage radius  $s_e$ . Consequently,  $P_{\text{LoS}}$  decreases, which in turn causes an increased path loss  $\text{PL}_m^e$ .

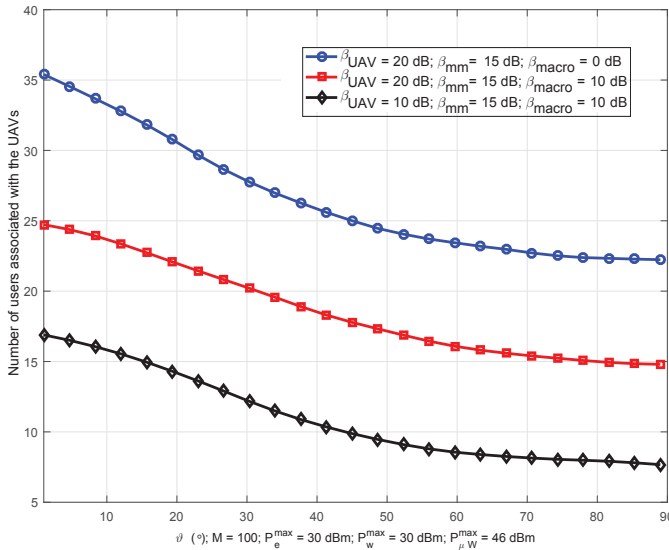


Fig. 3: User association for the UAV tier versus the half power beamwidth angle of the UAV.

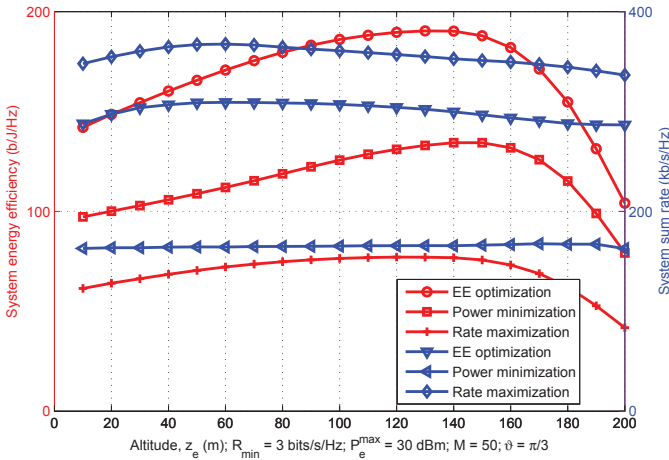


Fig. 4: System sum rate and system EE versus UAV altitude  $z_e$ .

This increased path loss experienced by transmissions reduces association with the UAV tier. Additionally, of the three graphs in Figure 3, the one representing the scenario with the highest  $\beta_{UAV}$  and lowest  $\beta_{macro}$  clearly outperforms the other two. For instance, the number of users associated with the UAV tier in the case involving a  $\beta_{macro}$  of 0 dB at  $\vartheta_{UAV} = 89^\circ$  is nearly three times that of the scenario with  $\beta_{UAV} = \beta_{macro} = 18$  dB.

Figure 4 describes the system sum rate and system EE versus UAV altitude  $z_e$ , for all power allocation mechanisms. The graphs for system EE demonstrate that our EE maximization approach outperforms the power minimization and rate maximization power allocation mechanisms. It is also obvious that the system EE reaches a maximum point at  $z_e = 140$  m, which corresponds to  $PL_{max} = 68.8$  dB. Beyond this altitude, the system EE begins to decrease. In fact, the system EE at  $z_e = 140$  m, using the EE maximization approach is 35% greater in comparison to  $z_e = 10$  m. Meanwhile, the system sum rate for the EE maximization approach reaches a

maximum point when  $z_e = 50$  m. It is shown that at higher UAV altitudes, while  $P_{LoS}$  increases,  $PL_m^e$  also increases due to an increased UAV-user distance. As a result of this all other simulations results are performed at  $z_e = 140$  m.

Figure 5 describes the system EE with or without the UAV tier, versus  $\tau = 2^{R_{min}} - 1$ . It is evident for the EE maximization approach that at  $\tau = 0$  dB, the system EE with a UAV tier is almost two times greater. Similarly, for the other two considered power allocation approaches, the advantages of including the UAV tier are quite evident from Figure 5.

Figure 6 depicts the system sum rate versus  $\tau$  with and without the UAV tier. The maximum achievable sum rate using the rate maximization approach with UAV tier is approximately 13% greater. The results for the other power allocation approaches are also higher when the system includes the UAV tier. For instance, at  $\tau = 20$  dB, the achievable sum rate for the power minimization approach is approximately 10% greater.

The variations in system EE and system sum rate versus  $\tau$  for all power allocation approaches is examined in Figure 7. The EE maximization approach outperforms the power minimization and rate maximization approaches in terms of system EE, expectedly. At  $\tau = -20$  dB, the system EE for the power minimization approach is approximately 88% lower. However, an increase in  $\tau$  subsequently results in an increase in the system EE for this approach and reaches a maximum point at  $\tau = 0$  dB. The achievable system EE for the rate maximization approach remains constant irrespective of the values of  $\tau$ . Additionally, as  $\tau$  takes higher values, greater transmission power is required to achieve the minimum required QoS level, which causes a decrease in the system EE shown by the EE maximization and power minimization approaches. The rate maximization approach achieves the highest sum rate for the considered values of  $\tau$  being investigated, as expected. At  $\tau = 30$  dB, the achievable system sum rate for the EE maximization and power minimization approaches is approximately equal to the achieved sum rate for the rate maximization approach.

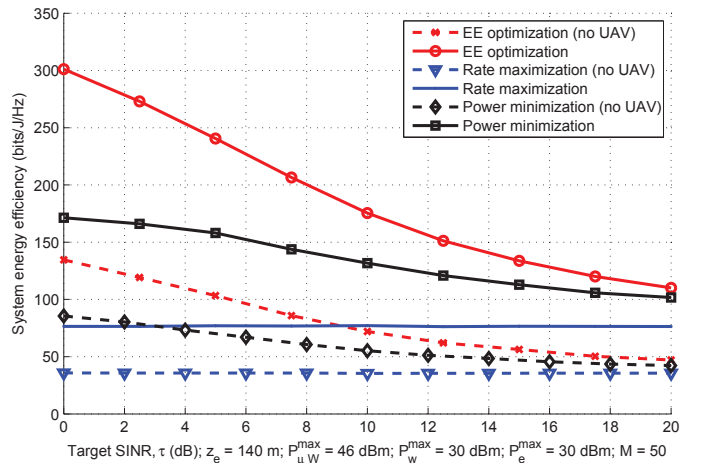


Fig. 5: System EE versus target SINR  $\tau$ , both with and without the UAV tier.

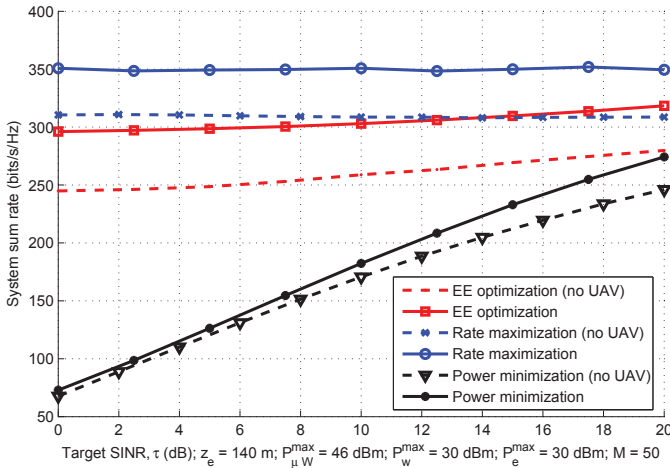


Fig. 6: System sum rate versus target SINR  $\tau$ , with and without UAVs.

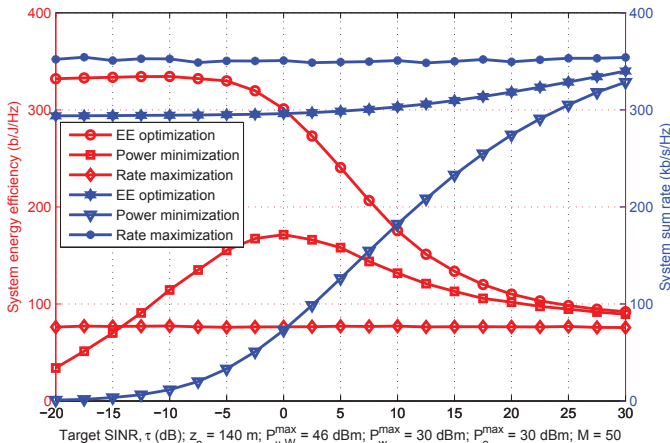


Fig. 7: System sum rate and system EE versus target SINR,  $\tau$ .

## VII. CONCLUSION

We designed an efficient radio resource management optimization framework for a multi-tier multi-band mmWave cellular network integrating UAV-based aerial small cells for enhanced coverage/throughput. We analyzed the system EE and system sum rate, along with other metrics, of this setting, where a varying number of users could be associated with the UAV tier depending on the biasing factors of all three network tiers. Our results demonstrate that including a UAV tier in the network can nearly double the system EE at certain target SINR values. Furthermore, we showed that the system EE increases with an increase in UAV altitude and after an optimal UAV altitude, it starts decreasing. Our results show that our proposed approach outperforms traditional schemes aimed at maximizing the system sum rate or minimizing the system power consumption.

## VIII. FUTURE WORK

The paper represents a motivating starting point for rich follow-up work that falls outside the scope of the paper. This includes complexity analysis and design of sub-optimal lower complexity methods, investigation of practical implementation

aspects, joint solution of power allocation and user association, and investigation of horizon-based dynamic UAV placement, and economics of UAV-enabled 5G network coverage.

## ACKNOWLEDGEMENT

We acknowledge the constructive comments of H. Pervaiz, S. A. Hassan, and Q. Ni on an earlier draft and the assistance of B. Girasolle on a mature version of the manuscript.

## REFERENCES

- [1] E. Hossain, et al., "Evolution toward 5G multitier cellular wireless networks: An interference management perspective," *Wireless Commun.*, vol. 21, no. 3, pp. 118-127, 2014.
- [2] R. Yaliniz, A. El-Keyi, and H. Yanikomeroglu, "Efficient 3-D placement of an aerial base station in next generation cellular networks," in *Proc. of IEEE Int'l Conference on Communications (ICC)*, May 2016.
- [3] I. Bucaille, S. Hethuin, A. Munari, R. Hermenier, T. Rasheed, and S. Allsopp, "Rapidly deployable network for tactical applications: Aerial base station with opportunistic links for unattended and temporary events absolute example," in *Proc. of IEEE Military Communications Conference*, San Diego, CA, USA, Nov. 2013.
- [4] A. Hourani, S. Kandeepan, and A. Jamalipour, "Modeling air-to-ground path loss for low altitude platforms in urban environments," in *Proc. of IEEE Global Communications Conf. (GLOBECOM)*, USA, 2014.
- [5] Q. Feng, J. McGeehan, E. K. Tameh, and A. R. Nix, "Path loss models for air-to-ground radio channels in urban environments," in *Proc. of IEEE Vehicular Technology Conference (VTC)*, Australia, 2006.
- [6] A. Al-Hourani, S. Kandeepan, and S. Lardner, "Optimal LAP altitude for maximum coverage," in *IEEE Commun. Letters*, vol. 3, no. 6, pp. 569-572, 2014.
- [7] M. Mozaffari, W. Saad, M. Bennis, and M. Debbah, "Drone Small Cells in the Clouds: Design, Deployment and Performance Analysis," in *Proc. of the IEEE Global Communications Conference (GLOBECOM), Wireless Networks Symposium*, San Diego, CA, USA, Dec. 2015.
- [8] M. Mozaffari, W. Saad, M. Bennis, and M. Debbah, "Optimal Transport Theory for Power-Efficient Deployment of Unmanned Aerial Vehicles," in *Proc. of the IEEE International Conference on Communications (ICC), Wireless Communications Symposium*, Malaysia, May 2016.
- [9] M. Chen, M. Mozaffari, W. Saad, C. Yin, M. Debbah, and C. Hong, "Caching in the sky: proactive deployment of cache-enabled unmanned aerial vehicles for optimized quality-of-experience," *IEEE J. Sel. Areas Commun.*, Vol. 35, No. 5, May 2017.
- [10] S. Singh, M. Kulkarni, A. Ghosh, and J. Andrews, "Tractable model for rate in self-backhauled millimeter wave cellular networks," *IEEE J. Sel. Areas Commun.*, vol. 33, no. 10, pp. 2196-2211, Oct. 2015.
- [11] O. Semiari, W. Saad, and M. Bennis, "Joint millimeter wave and microwave resources allocation in cellular networks with dual-mode base stations," *IEEE Trans. Wireless Communications*, vol. 16, no. 7, July 2017.
- [12] V. Sharma, M. Bennis, and R. Kumar, "UAV-Assisted heterogeneous networks for capacity enhancement," *IEEE Commun. Letters*, vol. 20, no. 6, pp. 1207 - 1210, 2016.
- [13] M. Omar, M. Anjum, S. Hasan, et al., "Performance Analysis of Hybrid 5G Cellular Networks Exploiting mmWave capabilities in suburban areas," in *Proc. IEEE Int'l Conf. Communications*, 2016.
- [14] N. Abuzainab and W. Saad, "Cloud radio access meets heterogeneous small cell networks: A cognitive hierarchy perspective," in *Proc. IEEE Int'l Workshop on Signal Processing Advances in Wireless Communications*, Edinburgh, UK, Jul. 2016.
- [15] H. Kuhn, "The Hungarian method for the assignment problem," *Naval Research Logistics Quarterly* 2, pp. 83-97, 1955.
- [16] T. Bai and R. Heath Jr., "Coverage and rate analysis for millimeter-wave cellular networks," *IEEE Trans. Wireless Communications*, vol. 14, no. 2, February 2015.